Particles in RSOS paths

2009 J. Phys. A: Math. Theor. 42 122001

(http://iopscience.iop.org/1751-8121/42/12/122001)

IOP FTC
IOP PUBLISHING JOURNAL OF PHYSICS A: MATHEMATICAL AND THEORETICAL

J. Phys. A: Math. Theor. **42** (2009) 122001 (14pp) doi:10.1088/1751-8113/42/12/122001

FAST TRACK COMMUNICATION

Particles in RSOS paths

P Jacob and P Mathieu

Département de Physique, de génie Physique et d'optique, Université Laval, Québec G1K 7P4, Canada

E-mail: patrick.jacob@hotmail.com and pmathieu@phy.ulaval.ca

Received 14 January 2009, in final form 11 February 2009
Published 2 March 2009
Online at stacks.iop.org/JPhysA/42/122001

Abstract

We introduce a new representation of the paths of the Forrester–Baxter restricted-solid-on-solid (RSOS) models which represents the states of the irreducible modules of the minimal models $\mathcal{M}(p', p)$. This representation is obtained by transforming the RSOS paths, for the cases $p \geqslant 2p' - 1$, to new paths for which horizontal edges are allowed at certain heights. These new paths are much simpler in that their weight is nothing but the sum of the position of the peaks. This description paves the way for the interpretation of the RSOS paths in terms of Fermi-type charged particles out of which the fermionic characters could be obtained constructively. The derivation of the fermionic character for $p' = 2$ and $p = kp' \pm 1$ is outlined. Finally, the particles of the RSOS paths are put in relation to the kinks and the breathers of the restricted sine-Gordon model.

PACS numbers: 11.25.Db, 02.10.Ox

1. Introduction

All the minimal models $\mathcal{M}(p', p)$ (where p and p' are coprime and $p > p'$) have a restricted-solid-on-solid (RSOS) path description. It means that the states in irreducible modules can be represented by the infinite-length limit of lattice paths, with the initial and final points characterizing the module. The link between the generating function of paths (or equivalently, configuration sums, since a path forms the contour of an RSOS configuration) and characters, discovered in [1], relies on the corner-transfer matrix solution [2] of the statistical model in the so-called regime III [3, 4].

The RSOS paths with parameters (p', p)—referred to as the RSOS(p', p) paths—provide thus a combinatorial description of the set of states of the $\mathcal{M}(p', p)$ model [5].

The fermionic character [6] of all irreducible modules can be derived from this path description [7]. However, the method used in these latter references does not make clear the particle structure of the generic RSOS(p', p) paths that underlies the fermionic character. This prevents a direct constructive (as opposed to a recursive) approach to these fermionic

forms. This is to be contrasted with the analysis of [8] for the special (and much simpler) class of unitary models ($p' = p - 1$). There, an RSOS path is interpreted as a closely packed configuration of one-dimensional charged fermionic-type particles with specific exclusion rules. The character is obtained constructively and expressed as a multiple-sum over the number of particles of different types.

There are two other classes of minimal models that do have a path representation with a neat particle description: the Yang–Lee sequence $\mathcal{M}(2, 2k + 1)$ [9] (following their analysis in [10]) and the $\mathcal{M}(k + 1, 2k + 3)$ [11] ones[1].

Here, we present a correspondence between RSOS(p', p) paths, for $p \geqslant 2p' - 1$, with a new type of paths, which we call generalized Bressoud paths, to be denoted as B(p', p). The original Bressoud paths [13] provide still another path description of the $\mathcal{M}(2, 2k + 1)$ models (combining the results of [10, 12, 13]). In addition to northeast (NE) and southeast (SE) edges—out of which RSOS paths are composed, horizontal (H) edges are allowed on the x-axis. For the generalized Bressoud paths B(p', p), H edges are allowed at specific heights, determined by the ratio p/p'. The crux of the matter with this transformation is that the weight of a B(p', p) path is simply the horizontal position of its peaks plus half the position of its 'half-peaks'. This is a key step for the reinterpretation of the collection of paths in terms of a gas of Fermi-type charged particles.

But what is meant by a *particle interpretation of a path*? If the paths can be decomposed into a number of building blocks whose dynamics (by which we refer to the block displacements and the interpenetration patterns of the blocks of different types) generate all possible paths, then we say that we have a particle interpretation, the particles being identified with the basic blocks. Typically the particles are elementary triangles, as in the unitary case or the $\mathcal{M}(2, 2k + 1)$ models, or generalized triangles incorporating some H edges, as observed in the new paths obtained here but also for the paths pertaining to the superconformal models [14]. The charge qualifier in the expression 'Fermi-type charged particles' refers to a label that distinguishes the different particles, usually related to the triangle width. Their ferminionc nature reflects the impenetrability of identical particles.

Our main point here is that the transformation of RSOS paths to generalized Bressoud paths is instrumental for reading off a natural set of particles. Once we have a particle description of a class of paths, it is usually possible to obtain their fermionic character by a direct constructive method. This is illustrated here for the general $\mathcal{M}(p', kp' \pm 1)$ models.

To which extent is this particle description physical? Granting its uniqueness, we expect these particles to be related to the (yet to be fully worked out) quasi-particles underlying a representation of the minimal-model irreducible modules. Such a representation would provide a substitute to the usual representation theory based on the Virasoro algebra and its singular vectors. But more immediately, this should match the particle description of the off-critical theory. The RSOS model in regime III provides an off-critical lattice description of the minimal models perturbed by the $\phi_{1,3}$ field [15], a perturbation that preserves integrability [16]. The spectrum of RSOS particles should thus be compared to that of these integrable models. This is addressed in section 5 where the RSOS particles are related to the kinks and the breathers of the restricted sine-Gordon model [18].

2. RSOS(p', p) paths

A configuration pertaining to the RSOS realization of the finitized $\mathcal{M}(p', p)$ minimal models (with $p > p'$) is described by a sequence of values of the height variables $\ell_i \in \{1, 2, \ldots, p-1\}$.

[1] T Welsh reported that he has found a bijection relating the path description of the $\mathcal{M}(k + 1, 2k + 3)$ models found in [11] to the standard RSOS paths (private communication).

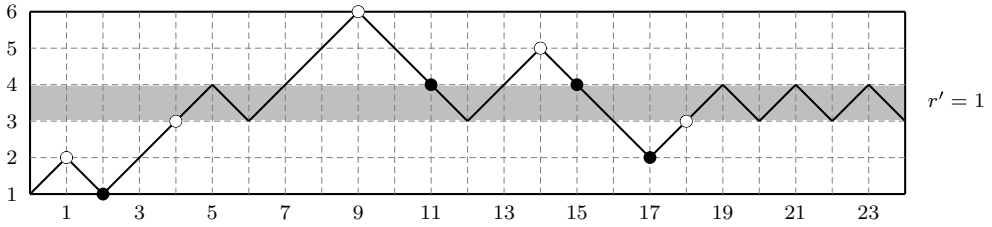

Figure 1. A typical path pertaining to the vacuum module ($s = r = 1$) for the $\mathcal{M}(2, 7)$ model (the identification of a module in terms of the end points is explained at the end of the section, in equation (8)). The weight $\tilde{w}$ of this path obtained using expression (2) is $\tilde{w} = 131/2$. The corresponding ground-state configuration is the path which starts with two NE edges and is followed by a sequence of 11 pairs of (NE,SE) edges. Its weight is $47/2$. The relative weight of the pictured path is thus $\Delta\tilde{w} = \tilde{w} - \tilde{w}_{\rm gsc} = 42$. The dots indicate the scoring vertices which refer to the alternative weight description of the path explained below in the main text. The white dots have weights u_i and the black ones have weights v_i, these being defined in equation (6). The scoring vertices have respective weights 0, 1, 1, 2, 7, 5, 9, 9, 8, so that the weight, w, of the path is $w = 42$, illustrating the identity $\Delta\tilde{w} = w$.

The height index is bounded by $0 \leqslant i \leqslant L$. Adjacent heights are subject to the admissibility condition: $|\ell_i - \ell_{i+1}| = 1$. A path is the contour of a configuration. It is thus a sequence of NE or SE edges joining the adjacent vertices (i, ℓ_i) and $(i + 1, \ell_{i+1})$ of the configuration. Each path is specified by particular boundary conditions: the values of ℓ_0 and those of ℓ_{L-1} and ℓ_L (the last two specify the RSOS ground state on which the configuration is built). For definiteness, we will choose $\ell_{L-1} = \ell_L + 1$ so that the paths all terminate with a SE edge.

The weight of a path is the sum of the weight of all its non-extremal vertices:

$$\tilde{w} = \sum_{i=1}^{L-1} \tilde{w}_i. \tag{1}$$

With each type of vertex specified by the triplet $(\ell_{i-1}, \ell_i, \ell_{i+1})$, we have—in regime III [4]:

$$\begin{aligned} &(h \mp 1, h, h \pm 1): \quad \tilde{w}_i = \frac{i}{2}, \\ &(h, h \mp 1, h): \quad \tilde{w}_i = \pm i \left\lfloor \frac{h(p - p')}{p} \right\rfloor, \end{aligned} \tag{2}$$

with $\lfloor u \rfloor$ standing for the largest integer smaller than u.

The rectangle delimiting the RSOS(p', p) paths can be made p'-dependent looking by coloring in gray the $p' - 1$ strips between those heights h and $h + 1$ for which [7]

$$\left\lfloor \frac{hp'}{p} \right\rfloor = \left\lfloor \frac{(h + 1)p'}{p} \right\rfloor - 1. \tag{3}$$

It is easily verified that the values of h which satisfy this condition are the following:

$$h_{r'} = \left\lfloor \frac{r'p}{p'} \right\rfloor \qquad \text{for} \quad 1 \leqslant r' \leqslant p' - 1. \tag{4}$$

The upper bound on r' follows from the condition $h \leqslant p - 1$. The band structure is symmetric with respect to the up–down reversal. For unitary models, $p = p' + 1$, all the bands are gray. In the other extreme case, for the $\mathcal{M}(2, p)$ models, there is a single gray band, right in the middle. The band structure is illustrated in figures 1–3 where basically the same path is drawn but within rectangles pertaining to the $\mathcal{M}(p', 7)$ models with $p' = 2, 3$ and 4.

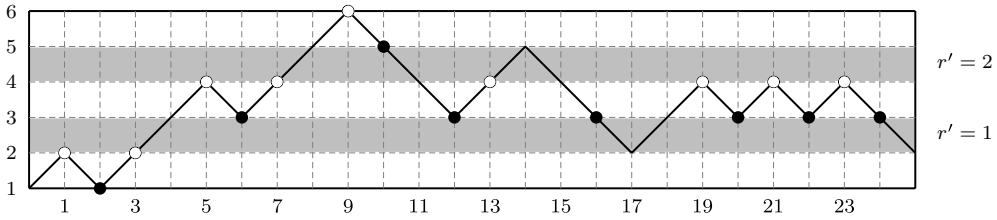

Figure 2. The path of figure 1 for the $\mathcal{M}(3, 7)$ model augmented with a SE edge, with its scoring vertices indicated. It again describes a state in the vacuum module $s = r = 1$. The corresponding ground-state configuration is the path with a single NE edge followed by a zigzag pattern in the first gray band. The relative weight of the pictured path is found to be $\Delta\tilde{w} = 92$.

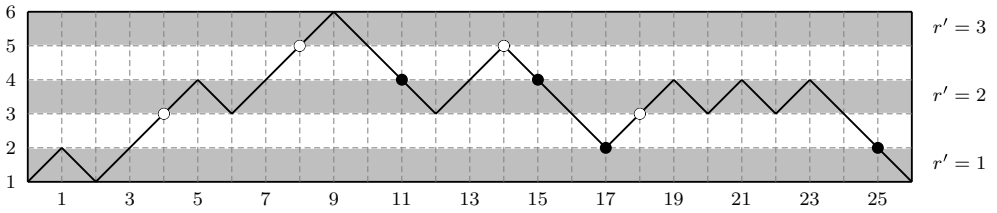

Figure 3. The path of figure 1 augmented with 2 SE edges, in the context of the $\mathcal{M}(4, 7)$ model. It represents a state in the vacuum module. If the path were cut at $L = 24$, it would instead correspond to a state in the module with $s = 1, r = 2$.

For reasons to be explained shortly, our analysis is restricted to those models for which the gray bands are isolated. This is so when

$$p \geqslant 2p' - 1. \tag{5}$$

For $p = 7$, the three cases illustrated are precisely those that satisfy this bound.

With the boundary conditions specified, there is a unique ground-state configuration defined to be the path with lowest weight. Let the weight of the ground-state configuration be $\tilde{w}_{\mathrm{gsc}}$. The relative weight of a path is $\Delta\tilde{w} = \tilde{w} - \tilde{w}_{\mathrm{gsc}}$. It is the relative weight which is related to the conformal dimension of the corresponding descendant state relative to the highest weight state (whose identification is given below).

An alternative weight prescription for RSOS paths, denoted by w, is presented in [7]. In the terminology of these references, a vertex is either scoring, with a non-zero weight u_i or v_i given by

$$u_i = \tfrac{1}{2}(i - \ell_i + \ell_0), \qquad v_i = \tfrac{1}{2}(i + \ell_i - \ell_0), \tag{6}$$

or non-scoring, meaning that it does not contribute to the weight. The scoring vertices of weight u_i are those where the path enters a gray band from below and the local maxima in white bands, while scoring vertices of weight v_i are those where the path enters a gray band from above and the local minima that are not in gray bands.

The scoring vertices for the three paths of figures 1–3 are indicated by white dots when their weight is u_i and by black dots if it is v_i. The pattern of scoring vertices (their number and their position) is manifestly very sensitive to the value of p'.

That relatively few vertices contribute to the weight w is a first important simplification. The second one is that both u_i and v_i are always non-negative (in contrast to the expression of

$\tilde{w}_i$ in (2)). Finally, this weight prescription is absolute: there is no need to subtract the weight of the ground state with the same boundaries:

$$\Delta\tilde{w} = \tilde{w} - \tilde{w}_{\rm gsc} = w. \tag{7}$$

It is clear from this new weight function that a weightless infinite tail—mandatory for a well-defined infinite length limit in which the conformal states are recovered—is a zigzag within a specific gray band. Since there are $p' - 1$ such bands, there are $p' - 1$ possible tails for the paths. Moreover, because every path is required to terminate with a SE edge, a path must thus end at the bottom of the band, at $\ell_L = \lfloor rp/p' \rfloor$, for some r within the range $1 \leqslant r \leqslant p' - 1$.

The proper relation between (ℓ_0, ℓ_L) and the irreducible indices (r, s), where $1 \leqslant r \leqslant p' - 1$ and $1 \leqslant s \leqslant p - 1$, is the following:

$$\ell_0 = s, \qquad \ell_L = \left\lfloor \frac{rp}{p'} \right\rfloor. \tag{8}$$

Clearly, the ground-state path with s, r given is the shortest path starting from s that reaches the rth gray band and it is easily checked that it has $w = 0$.

The path generating function with specified boundaries is

$$X^{(p',p)}_{\ell_0,\ell_L}(q; L) = \sum_{\substack{\text{paths with fixed end} \\ \text{points } \ell_0 \text{ and } \ell_{\rm L}=\ell_{\rm L-1}-1 \\ \text{and } L=\ell_0+\ell_L \bmod 2}} q^w. \tag{9}$$

With this identification, $X^{(p',p)}_{\ell_0,\ell_L}(q)$ is the finitized version of the Virasoro characters $\chi^{(p',p)}_{r,s}(q)$. The full character is recovered in the limit $L \to \infty$:

$$\chi^{(p',p)}_{r,s}(q) = \lim_{L\to\infty} X^{(p',p)}_{s,\lfloor rp/p' \rfloor}(q; L). \tag{10}$$

3. From RSOS(p', p) to B(p', p) paths

We are now in a position to formulate the bijection between RSOS(p', p) paths to generalized Bressoud—or B(p', p)—paths. The operations defining the correspondence from RSOS(p', p) to B(p', p) paths are as follows:

- Flatten the $p' - 1$ gray bands.
- Fold the part of the strip below the first gray band ($1 \leqslant h \leqslant h_1$) onto the region just above it ($h_1 + 1 \leqslant h \leqslant 2h_1$).
- Reset the starting height to 0.

In the flattening process, all SE and NE edges within the gray bands are mapped into H ones. It is thus crucial for the reconstruction of the RSOS path by the inverse operation that the gray bands be isolated. It is only in this way that one can recover a unique zigzag pattern in a gray band from a sequence of H edges. Gray bands are isolated when condition (5) is satisfied. Our analysis is thus restricted to those classes of models. Note also that the folded part can never overlap with the second gray band.

The new paths are defined in the strip $0 \leqslant x \leqslant L$ and $0 \leqslant y \leqslant y_{\rm max}$ with

$$y_{\rm max} = p - p' - \left\lfloor \frac{p}{p'} \right\rfloor. \tag{11}$$

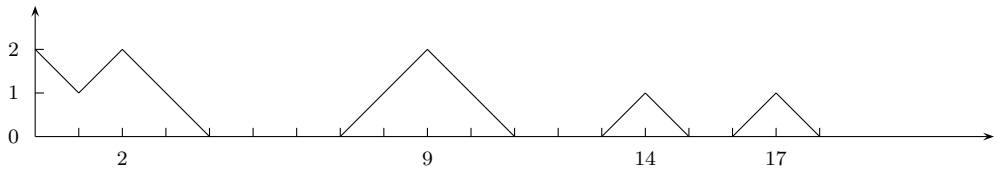

Figure 4. The transformation of the RSOS(2, 7) path of figure 1 into a B(2,7) path.

In these Bressoud-type paths, H edges are allowed at all heights $y(r')$, with $1 \leqslant r' \leqslant p' - 1$ given by

$$y(r') = \left\lfloor \frac{r'p}{p'} \right\rfloor - \left\lfloor \frac{p}{p'} \right\rfloor - r' + 1. \tag{12}$$

A path terminates at one of the heights $y(r')$, namely that with $r' = r$.

The origin of H edges as RSOS edges within the gray bands places some restrictions on the parity of the number of successive H edges at a given height > 0. If the sequence of H edges is separated by edges of the same type (either both NE or SE), then the number of successive H edges must be odd. It is even otherwise. In other words, if ℓ and ℓ' are the height of the vertices before and after those linked by the sequence of H edges, the number of H edges has the same parity as $|\ell - \ell'|/2$.

The flattening and the folding processes make the definition of the boundary conditions at the beginning of the $B(p', p)$ path somewhat complicated in general, although these are easily read off the original RSOS path. For instance, if $s = 1$ and $p > 2p' - 1$ (meaning that the RSOS rectangle does not have a gray band starting at $h = 1$), the $B(p', p)$ path starts with a SE edge at $y_0 = h_1 - 1$. Moreover, there is a constraint on the initial point i_0 of the first H edge, which is $i_0 = h_1 - 1 \bmod 2$. Similarly, if $s = 1$ and $p = 2p' - 1$, the first edge in the generalized Bressoud path is an H edge on the x-axis.

Finally, the weight $\hat{w}$ of these new paths is computed from the sum of the x-position of its peaks and half the x-position of its half-peaks:

$$\hat{w} = \sum_{\text{peaks}} i + \frac{1}{2} \sum_{\text{half-peaks}} i. \tag{13}$$

A half-peak is a vertex in-between (NE, H) or (H, SE) edges.

For a path with given boundaries $y_0 = s$ and $y_L = y(r)$, the weight must be renormalized (by a simple subtraction) relative to the ground-state configuration pertaining to these end points:

$$\Delta\hat{w} = \hat{w} - \hat{w}_{\text{gsc}} = w. \tag{14}$$

The generalized Bressoud paths corresponding to the three RSOS paths of figures 1–3 are illustrated in figures 4–6.

The bijective nature of this correspondence is clear. On one hand, the transformation of an RSOS to a generalized Bressoud path is manifestly unique. On the other hand, the reverse procedure is also unambiguous. With both L and the nature of the last edge (SE) fixed, the RSOS path is uniquely recovered from a B path, starting from the end (since the folding does not induce an ambiguity on the end point). In this reverse operation, each line where there are allowed values for the H edges is transformed into a gray band: H edges become zigzag patterns within gray bands.

The crucial point is the demonstration of the weight preserving character of the bijection, namely, the proof of (14). To present the key point without the complications induced by the

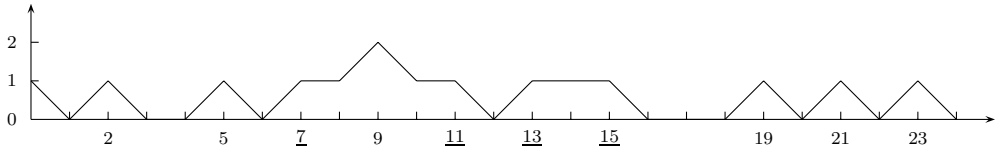

Figure 5. The B(3,7) path corresponding to the RSOS(3,7) path of figure 2. Here, H edges are allowed at $y = 0, 1$ but not $y = 2$. The horizontal positions that are underlined indicate the positions of the half-peaks.

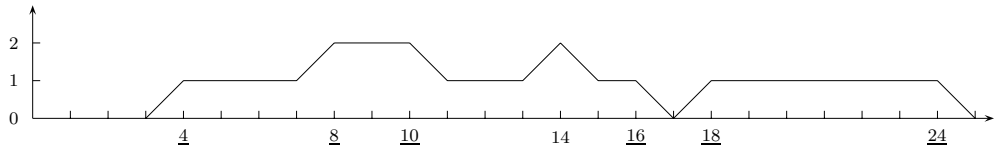

Figure 6. The B(4,7) path corresponding to the RSOS(4,7) path of figure 3. Here, H edges are allowed at all values of $y \leqslant 2$. The horizontal positions that are underlined indicate the positions of the half-peaks.

boundary effects, let us restrict to the case $s = r = 1$, for which $\hat{w}_{\rm gsc} = 0$. What has to be shown then is that $w = \hat{w}$. This is demonstrated in terms of a pairing of the scoring vertices of different types, from right to left and in a nested way (meaning that adjacent unlike scoring vertices are paired first, as clarified in the examples below). If the scoring vertices have height $\ell_i > h_1$, the pairing starts (at the right) with a $\bullet$ vertex; this is called a type-1 pairing. A type-2 pairing occurs when the two vertices are below the first gray band; in that case, the pairing starts with a $\circ$-type vertex. With the specified boundaries, all scoring vertices come in pairs except for an isolated $\circ$ at the beginning of the path (if $p > 2p' - 1$), whose weight is 0 (and such an unpaired vertex is absent when $p = 2p' - 1$).

For the path of figure 1, the pairing is as follows: $\circ(\bullet\circ)(\circ\bullet)(\circ\bullet)(\bullet\circ)$. All pairings are between nearest neighbors. For the path of figure 2, the pairing is $\circ(\bullet\circ)(\circ\bullet)(\circ(\circ\bullet)\bullet)(\circ\bullet)(\circ\bullet)$ $(\circ\bullet)(\circ\bullet)$. In this case, there is a nested pairing: the $\circ$ vertex at 7 is paired with the $\bullet$ vertex at 12 and these are separated by a pair $(\circ\bullet)$. A non-nearest-neighbor pairing occurs when the path in-between the two scoring vertices crosses one or more gray bands. For the path in figure 3, the pairings are $(\circ(\circ\bullet)(\circ\bullet)\bullet)(\circ\bullet)$: the $\circ$ vertex at 4 is paired with the $\bullet$ one at 17.

If a pair is not separated by a zigzag pattern in a gray band, it is mapped (via the bijection) to a peak centered at the position i of the leftmost scoring vertex of the pair. If there is an in-between zigzag pattern in a gray band of length 2β (which is possible only for type-1 pairing), then the pair is replaced by a pair of half-peaks, one at i and the other at $i + 2\beta$. The different possibilities are illustrated in figure 7.

The correspondence just indicated is supported by the verification of the identity $w = \hat{w}$. Consider a pairing of the first type, with the vertices $(\circ, \bullet)$ at respective position (i, ℓ_i) and $(i + a, \ell_i - a)$, so that

$$u_\circ = \frac{i - \ell_i + 1}{2}, \qquad v_\bullet = \frac{i + a + (\ell_i - a - 1)}{2} \quad \Rightarrow \quad w_{(\circ,\bullet)} = u_\circ + v_\bullet = i, \tag{15}$$

which is the weight of the Bressoud peak at position i (cf figure 7(*a*)). In the more general case where the two scoring vertices are separated by a zigzag pattern of length 2β, one has

$$u_\circ = \frac{i - \ell_i + 1}{2}, \qquad v_\bullet = \frac{i + a + 2\beta + (\ell_i - a - 1)}{2} \quad \Rightarrow \quad w_{(\circ,\bullet)} = u_\circ + v_\bullet = \frac{i}{2} + \frac{i + 2\beta}{2}. \tag{16}$$

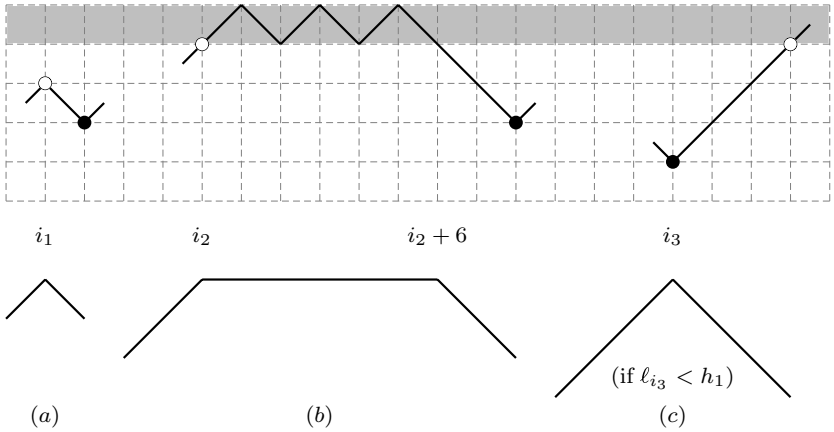

Figure 7. The different types of pairing of two scoring vertices that make a peak, or two paired half-peaks, in the corresponding generalized Bressoud path. The first two cases describe pairings of type 1, that is of the form $(\circ, \bullet)$. In (a) the two scoring vertices are adjacent local extrema. The two vertices 'fuse' in the Bressoud path into a simple peak. The height of this peak is given by the height difference between the two scoring vertices, here 1. The position of the peak is that of the $\circ$ vertex. In (b), the two vertices are separated by a gray-band zigzag pattern of length 6. The corresponding half-peaks are separated by 6 H edges. The positions of the half-peaks are at the extremities of the zigzag pattern, namely at the position of the $\circ$ and that of the $\bullet$ minus the height difference, which is 2 here. This height difference is the height of the resulting flattened peak. The case (c) describes a situation that is possible only if the two scoring vertices lie below the first gray band (with $r' = 1$). They both fuse into a peak (due to the folding process) and the peak position is that of the $\bullet$ vertex. Its height is 3, the height difference of the two scoring vertices.

Here the total weight $i + \beta$ is written in the form of two contributing half-peaks, at i and $i + 2\beta$ (cf figure 7(b)). In both cases, the pair of scoring vertices is found to describe a peak of height a, which is flattened if $\beta > 0$. The computation for a case where there are in-between pairs of scoring vertices is similar. In such a case, the path leaves the gray band from above, instead of simply zigzagging within it; there will then necessarily be at least one pair of unlike scoring vertices in the portion of the path above the gray band under consideration. The result of the computation is the same as above, with 2β being defined more precisely as the distance between the gray band entry point (the position of the $\circ$ vertex) and its exit point in the downward direction.

When the pairing is of the form $(\bullet, \circ)$, with the scoring vertices at respective positions (i, ℓ_i) and $(i + a, \ell_i + a)$, with $\ell_i + a \leqslant h_1$ (since for that type of pairing the two vertices must lie below the first gray band), $w_{(\bullet,\circ)} = i$; the peak in the B path is centered at i (cf figure 7(c)).

This analysis shows that pairs of scoring vertices can be put in correspondence with peaks or pairs of half-peaks and that this correspondence is weight preserving. This completes the proof of the identity $w = \hat{w}$ for $s = r = 1$.

4. Sample B(p', p) particle spectra and generating functions

We identify here the particle spectrum of some classes of B paths and outline the derivation of their generating function along the lines of [8] (see also [11, 14]). The resulting fermionic forms are given for the vacuum module and in the limit $L \to \infty$. The detail of these derivations will be presented elsewhere, together with the analysis of the additional modules.

4.1. $B(2, 2k+1)$ paths

As already said, an RSOS$(2, 2k+1)$ path is defined within a rectangle having a single gray band in its center. In the transformation, this band is flattened out, the part of the strip below the gray band is folded onto the one above it, and the height $h = k+1$ is reset to $y = 0$. By construction, this new path has peaks with height $\leqslant k-1$. These peaks are either at the positions of the peaks in the portions of the RSOS$(2, 2k+1)$ path which lie above the gray band or at the positions of the valleys below it. In addition, the B$(2, 2k+1)$ paths might contain possible H edges on the horizontal axis: these are the edges that originally lay within the gray band. Clearly, the resulting paths have all the characteristics of Bressoud paths[2].

Note that for this special case, a weight-preserving bijection is known to exist (combining the results of [13, 20]). Once the relationship between the two types of paths is unraveled, it follows that the correspondence must be weight preserving. This provides an alternative proof of the identity $w = \hat{w}$ for that case (and which applies here to all values of s).

Now, the Fermi-gas analysis of the Bressoud paths is straightforward[3]. The particles are the peaks of height $1 \leqslant y \leqslant k-1$. We let the height of an isolated peak be its charge. Let m_j be the number of peaks of charge m_j in the path. With a fixed set of values $\{m_j\}$, the first step is to determine the configuration of minimal weight. Here it corresponds to the case where all the peaks are ordered in increasing value of the charge. The corresponding weight is $mBm + Cm$ in the expression below. Then, we determine the possible displacements of each type of peaks subject to two rules: particles with the same charge do not penetrate and particles of different charge can penetrate each other as long as they do not generate higher charged particles. In the present case, the presence of other types of particles does not affect the displacements of a particle of a given charge and each displacement of one step increases the weight by 1. To each type of particle, there is thus a factor $(q)_{m_j}^{-1}$. Then one sums over all values of $m_j \geqslant 0$. This leads directly to the fermionic character [10]:

$$\chi_{1,1}^{(2,2k+1)}(q) = \sum_{m_1,\cdots,m_{k-1}} \frac{q^{mBm+Cm}}{(q)_{m_1}\cdots(q)_{m_{k-1}}}, \tag{17}$$

where

$$(q)_m = \prod_{i=1}^{m}(1-q^i), \qquad B_{i,j} = \min(i, j) \quad \text{and} \quad C_j = j. \tag{18}$$

4.2. $B(p', kp'-1)$ paths

We now consider a natural extension of the previous class of models, the minimal models $\mathcal{M}(p', kp'-1)$, with $k > 1$. When $p = kp'-1$, the RSOS defining rectangle has a completely regular band structure: there are $k-2$ white bands at the borders of the rectangle (below the first gray band and above the last gray band) and two consecutive gray bands are separated by $k-1$ white bands. This class of models incorporates the limiting case $p = 2p'-1$ and figure 3 illustrates its band structure when $p' = 4$.

[2] We noted afterward—and with insight—that this bijection (without the folding operation) is also pointed out in [19] for the special case of the $\mathcal{M}(2, 5)$ model.

[3] It is spelled out in [9] in terms of a different type of paths. However, the analysis of [8] is readily adapted to Bressoud paths. Moreover, although the generating function in [13] is obtained by an inductive argument (which is thus a verification proof rather than a constructive one), it contains the key features for the constructive Fermi-gas derivation.

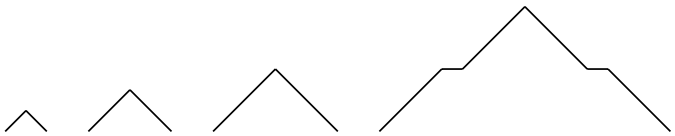

Figure 8. The four basic particles for the B(5, 14) path (of the class $(p', kp'-1)$ with $p'=5$ and $k=3$). The first two are labeled by the set I and the last two by the set I' in (19). H edges are allowed at heights 0, 3 and 6.

The corresponding $B(p', kp'-1)$ paths can be decomposed into a sequence of $p'+k-4$ particles labeled by $j=1,\ldots,p'+k-4$ and these are naturally separated into two sets:

$$I=\{1,\ldots,k-2\} \qquad \text{and} \qquad I'=\{k-1,\ldots,p'-k-4\}. \tag{19}$$

The first set of $k-2$ particles is defined as in the $B(2,2k-1)$ case: these are triangles of height j, with $j\in I$. For the other particles, it is convenient to define $j'=j-k+2$, so that $1\leqslant j'\leqslant p'-2$. The corresponding particles are represented by deformed symmetric triangles of height $j'(k-1)$ and whose left side has j' sequences $k-1$ NE edges all separated by an H edge. The top is a peak at height $j'(k-1)$, a height where H edges are allowed. It is thus convenient to view the top peak as being composed of two half-peaks. In addition to these, the particle labeled by j' contains $2(j'-1)$ other half-peaks due the presence of internal H edges. See for instance figure 8 where the particles for $p'=5, k=3$ are pictured; in that case, there are two particles of each type.

In the minimal-weight configuration (for a fixed particle content $\{m_j\}$), the particles are ordered by increasing values of $j\in I\cup I'$.

Each type of particles has a different dynamics. For those labeled by $j\in I$, the displacements are free (the presence of other particles of either type does not induce constraints) and they are described by the factor $(q)_{m_j}^{-1}$. This is as for the $B(2,2k-1)$ particles. The dynamics of the other types of particles is best regarded in terms of that of the half-peaks, taken collectively. Every half-peak is allowed to be displaced by 2 units, with a weight difference of 1. Let p_{k-2} be the number of half-peaks, where p_j is defined as follows:

$$p_j=2m_{j+1}+4m_{j+2}+\cdots+2(p'+k-3-j)m_{p'+k-4} \qquad \text{for} \quad j+1\in I'. \tag{20}$$

The displacements of all half-peaks are governed by the factor $(q)_{p_{k-2}}^{-1}$. However, this does not capture all possible configurations. Given a configuration with a specific set of positions for the various half-peaks, it is still possible to move half-peaks in-between the configuration under consideration—maintaining the two extremal (the first and the last) half-peaks fixed—such that each basic displacement increases the weight by 1. A basic displacement typically involves the opposite displacements of two half-peaks. The resulting configurations are most simply described in terms of the different penetration patterns of smaller particles (but still within the set I') into larger ones. All these possibilities are taken into account by the product of q-binomials in the expression below.

For instance, with the edges NE, SE and H represented respectively by 1, $\bar{1}$ and 0, the three configurations with $m_3=m_4=1$, regarded e.g. as B(5,14) paths (cf figure 8), are

$$\begin{aligned}
&111\bar{1}\bar{1}\bar{1}1110111\bar{1}\bar{1}\bar{1}0\bar{1}\bar{1}\bar{1}\\
&1110111\bar{1}\bar{1}\bar{1}111\bar{1}\bar{1}\bar{1}0\bar{1}\bar{1}\bar{1}\\
&1110111\bar{1}\bar{1}\bar{1}0\bar{1}\bar{1}\bar{1}111\bar{1}\bar{1}\bar{1}.
\end{aligned} \tag{21}$$

A peak (=two half-peaks) is the vertex in-between $1\bar{1}$ and a half-peak is either in-between 10 or $0\bar{1}$. A configuration is obtained from the previous one by displacing one half-peak forward

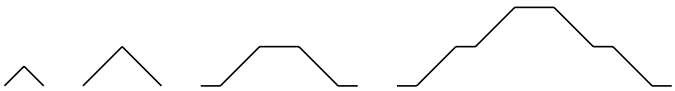

Figure 9. The four basic particles for the B(4, 13) paths (of the class $(p', kp'+1)$ with $p'=4$ and $k=2$). The second and the third particles both have height 2 but they differ in that the third one can be opened at its top but not the second one. Here H edges are allowed at heights 0, 2 and 4.

by 4 units and another one backward by 2 units, for a weight difference of 1. The results are taken into account by the q-deformation of the binomial factor $\binom{3}{1}$ defined below.

The vacuum character resulting from the analysis just sketched reads

$$\chi_{1,1}^{(p',p'k-1)}(q) = \sum_{m_1,\dots,m_{p'+k-4}} \frac{q^{mBm+Cm}}{(q)_{m_1}\cdots(q)_{m_{k-2}}(q)_{p_{k-2}}} \prod_{i=k-1}^{p'+k-5} \begin{bmatrix} m_i+p_i \\ m_i \end{bmatrix}, \tag{22}$$

where p_j is defined above. $B_{i,j}$ is the symmetric matrix whose entries, with $i \leqslant j$, are

$$B_{i,j} = \begin{cases} i & \text{for} \quad i,j \in I \\ ij' & \text{for} \quad i \in I,\ j \in I' \\ (i'k-1)j' & \text{for} \quad i,j \in I', \end{cases} \qquad \text{and} \qquad C_j = \begin{cases} j & \text{for} \quad j \in I \\ (k-1)j' & \text{for} \quad j \in I'. \end{cases} \tag{23}$$

(Recall that $j' = j-k+2$.) Finally, the q-binomial is defined as

$$\begin{bmatrix} a \\ b \end{bmatrix} = \begin{cases} \dfrac{(q)_a}{(q)_{a-b}(q)_b} & \text{if} \quad 0 \leqslant b \leqslant a, \\ 0 & \text{otherwise.} \end{cases} \tag{24}$$

We stress that this fermionic-character expression is not new [7] but it is written there in terms of the variables p_j (relabeled p_{j+1}) instead of m_j for $j \in I'$ (see also [17] corr 1.6, but pertaining to a different module, which entails minor modifications). However, its dressing with a particle interpretation is new.

4.3. $B(p', kp'+1)$ paths

To exemplify the non-triviality of the particle decomposition, we present the results for a related sequence, namely, $p = kp'+1$, with $k > 1$. The band structure still follows a simple pattern: there are now $k-1$ white bands below the first gray band and two consecutive gray bands are again separated by $k-1$ white bands. The generalized Bressoud paths are described in terms of $p'+k-3$ particles, naturally divided into two sets, labeled by I and I' defined as before in (19) but with $k \to k+1$. The first $k-1$ particles again correspond to triangles of height j, with $1 \leqslant j \leqslant k-1$. The other particles, with $j = k-1+j'$, correspond to deformed and flattened symmetric triangles of height $j'(k-1)$ and whose left side has j' sequences of $k-1$ NE edges, all separated by an H edge. In addition, these particles are topped by two H edges and they start and end with an H edge. See figure 9 for the representation of the particles of the B(4, 13) paths.

For the minimal-weight configuration, the particles are ordered by increasing values of $j \in I$ and then by decreasing values of $j \in I'$. The rest of the analysis is similar to that sketched in the previous case and results in

$$\chi_{1,1}^{(p',p'k+1)}(q) = \sum_{m_1,\cdots,m_{p'+k-3}} \frac{q^{mBm+Cm}}{(q)_{m_1}\cdots(q)_{m_{k-1}}(q)_{p_{k-1}}} \prod_{i=k}^{p'+k-4} \begin{bmatrix} m_i+p_i \\ m_i \end{bmatrix}, \tag{25}$$

where p_j is defined as before but with $k \to k+1$. The form of the symmetric matrix $B_{i,j}$ is as in (23) except for the third condition which reads: $B_{i,j} = i'(j'k+1)$ if $i \leqslant j$ and $i, j \in I'$. Finally, C is again given by equation (23). Again this expression is known [7] (see also the second reference in [6] section 4.4 and cf [17] corr 1.8), but its particle interpretation is new.

5. Particles versus kinks and breathers

In the previous section, we have unraveled the particle content of RSOS$(p', kp' \pm 1)$ paths. We expect the gross features of this spectrum to be generic to models with $p \geqslant 2p' - 1$. These features are the following. There are basically two types of particles. Type-*a* particles are those which can live in the white bands of the RSOS path that are below the first gray band (and they appear there as valleys). This defining domain is not exclusive (they can be seen elsewhere) but it is a precise characterization: the other particles cannot live there. The number of type-*a* particles is thus $h_1 - 1 = \lfloor p/p' \rfloor - 1$. In the corresponding Bressoud path, they are represented by triangles of height $1 \leqslant y \leqslant \lfloor p/p' \rfloor - 1$; these particles cannot be deformed by the insertion of H edges.

Type-*b* particles, on the other hand, are triangles that link two gray bands in the RSOS path. Each such particle is thus built up from sequences of NE and SE edges interpolating between two adjacent gray bands. As there are $p' - 1$ gray bands, there are thus $p' - 2$ such interpolating segments. Since the gray bands represent the possible RSOS vacua, type-*b* particle constituents can be viewed as fundamental kinks or antikinks interpolating between adjacent vacua. Particles of type-*b* are thus composed of j' kinks and j' antikinks, with $1 \leqslant j' \leqslant p' - 2$. In the Bressoud path context, a kink (antikink) interpolates between two successive heights where H edges are allowed and, in a fundamental particle, two adjacent kinks (antikinks) are separated by an H edge.

The characteristic property of type-*b* particles in B paths is that they can be deformed by the introduction of an even number of H edges at every height where such edges are allowed (and in particular, at their top); in other words, after any kink or antikink constituent segment, pairs of H edges can be introduced. This means that the constituent kinks and antikinks can be separated at will: they do not form bound states. A kink (antikink) component of a type-*b* particle actually corresponds to a half-peak toward the right (left). In contrast, particles of type *a* appear to describe genuine bound states, i.e. two confined half-peaks.

As mentioned in the introduction, the RSOS(p', p) model in regime III provides an integrable off-critical (lattice) description of the $\phi_{1,3}$-perturbed minimal model $\mathcal{M}(p', p)$. Its scaling limit is the restricted sine-Gordon equation at coupling $\beta^2/8\pi = p'/p$ [18]. This model has $p' - 1$ vacua, hence $p' - 2$ kinks (and as many antikinks). Moreover, there are $\lfloor p/p' \rfloor - 1$ bound states or breathers (see e.g. [21]). This matches the above counting: particles of type *a* are similar to breathers and those of type *b* are like composite of j' kinks and antikinks, or equivalently, pairs of kink–antikink of topological charge j'.[4]

6. Conclusion

We have presented a bijection between the RSOS paths and new generalized Bressoud paths for the class of models with $p \geqslant 2p' - 1$. In those cases, we have essentially provided a third

[4] Note that the perfect pairing between the number of kinks and antikinks encountered in most of our examples is a special feature of the condition $s = r$ (=1 for the vacuum module). For paths with $s \neq r$, there will be an excess of kinks or antikinks, neat evidence that they are not confined, even loosely. But note that these are the pairs of kink–antikink of charge j' that enter in the particle description of the fermionic forms, the excess being treated as a boundary effect.

weight function for the RSOS paths. The genuine advantage of this transformation of the RSOS paths to Bressoud-type ones, beyond the simplicity of the resulting weight expression, is that it marks out the way for a particle interpretation of the RSOS paths, which in turn should make possible the construction of their generating function (i.e., the character) by direct Fermi-gas-type method. This has been illustrated here for the $\mathcal{M}(p', kp' \pm 1)$ minimal models and remains to be worked out in full generality.

The particle spectrum that emerges naturally from the Bressoud path formulation—at least in its gross features abstracted from the cases studied explicitly—has been interpreted as the conformal limit of the solitons and breathers spectrum of the restricted sine-Gordon model at $\beta^2/8\pi = p'/p$. This matching provides neat support to the idea that fermionic forms capture the physics of a particular integrable perturbation and that its underlying quasi-particles should correspond to the massless limit of the particles of the off-critical theory (see, e.g. [6]).

The present analysis is restricted to the cases $p \geqslant 2p' - 1$. From the finitized characters of the models with $p > 2p'$, the finitized characters of those with $p < 2p'$ can be obtained by duality [7, 22]. Alternatively, for $p < 2p'$, there is a dual version of the transformation of the RSOS paths to the generalized Bressoud ones, but with a somewhat more complicated weight function. This will be considered elsewhere. But note that for those cases, there are no breathers in the spectrum since the bordering bands of the RSOS defining rectangle are always gray (or equivalently, all white bands are isolated).

Acknowledgments

PM acknowledges useful discussions with A LeClair and T Welsh. We also thank T Welsh for his critical comments on the article. Part of this work was done during the workshop *Low-Dimensional Quantum Field Theories and Applications* at the Galileo Galilei Institute for Theoretical Physics. PM thanks the GGI for its hospitality and the INFN for partial support during his stay. This work is supported by NSERC.

References

[1] Date E, Jimbo M, Kuniba A, Miwa T and Okado M 1987 *Nucl. Phys.* B **290** 231–73
[2] Baxter R J 1982 *Exactly Solved Models in Statistical Mechanics* (New York: Academic)
[3] Andrews G E, Baxter R J and Forrester P J 1984 *J. Stat. Phys.* **35** 193–266
[4] Forrester P J and Baxter R J 1985 *J. Stat. Phys.* **38** 435–72
[5] Melzer E 1994 *Int. J. Mod. Phys.* A **9** 1115–36
[6] Kedem R, Klassen T R, McCoy B M and Melzer E 1993 *Phys. Lett.* B **304** 263–70
Kedem R, Klassen T R, McCoy B M and Melzer E 1993 *Phys. Lett.* B **307** 68–76
[7] Foda O, Lee K S M, Pugai Y and Welsh T A 2000 *Contemp. Math.* **254** 157–86
Foda O and Welsh T A 2000 *Prog. Comb.* **191** 49–103
Welsh T 2005 *Memoirs of the American Mathematical Society* vol 827 (Providence, RI: American Mathematical Society)
[8] Warnaar S O 1996 *J. Stat. Phys.* **82** 657–85
[9] Warnaar S O 1997 *Commun. Math. Phys.* **184** 203–32
[10] Feigin B L, Nakanishi T and Ooguri H 1992 *Int. J. Mod. Phys.* A **7** 217–38
[11] Jacob P and Mathieu P 2007 *J. Stat. Mech.* P11005
[12] Burge W H 1981 *Discrete Math.* **34** 9–15
[13] Bressoud D 1987 *Lecture Notes Math.* **1395** 140–72
[14] Jacob P and Mathieu P 2008 *Nucl. Phys.* B **805** 517–44
[15] Huse D A 1984 *Phys. Rev.* B **30** 3908–15
[16] Zamolodchikov A B 1989 *Adv. Stud. Pure Math.* **19** 641–74
[17] Foda O and Quano Y-H 1997 *Int. J. Mod. Phys.* A **12** 1651–76

[18] LeClair A 1989 *Phys. Lett.* B **230** 103–7
Smirnov F A 1989 *Int. J. Mod. Phys.* A **4** 4213–20
Smirnov F A 1990 *Nucl. Phys.* B **337** 156–80
[19] Welsh T 2006 *J. Phys: Conf. Ser.* **30** 119–32
[20] Andrews G E, Baxter R J, Bressoud D M, Burge W H, Forrester P J and Viennot G 1987 *Eur. J. Comb.* **8** 341–50
[21] Zamolodchikov A B and Zamolodchikov Al B 1979 *Ann. Phys.* **120** 253–92
[22] Berkovich A and McCoy B M 1996 *Lett. Math. Phys.* **37** 49–66